

ENHANCING SNAKES FOR VESSEL DETECTION IN ANGIOGRAPHY IMAGES

Ricardo Toledo, Ramón Baldrich, Ernest Valveny, Petia Radeva
Computer Vision Center, Universitat Autònoma de Barcelona
08193 Bellaterra - Barcelona
Spain

Abstract

This paper proposes enhancements to the deformable models. Focusing on the problem of vessel segmentation, two general methods for improving the performance of the snakes are explained.

The snake framework has a critical step when using the energy minimising scheme applied to the segmentation problem in computer vision: the potential map is based on the output of a low level feature detection over the original image, and therefore, the whole method, being theoretically sound and correct, is highly dependent on the quality of the image feature detector used to build the potential field. To avoid these problems we propose a statistical vessel learning for an optimal feature detection. The knowledge can be either embedded into the minimizing scheme or used within the traditional framework.

Key Words: Deformable models, feature detection, statistical learning.

1. Introduction

When the objective is to extract boundary elements belonging to the same structure and integrate these elements into a coherent and consistent model of the structure, using deformable models is a natural way to regularize the ill-posed problem of segmentation and interpretation of images. Models have been used to guide pattern recognition systems [7, 8] but all of them are dependent, sooner or later, on some kind of conventional edge detection and, so, subject to its properties. By its own nature coronary vessels angiography shows a flexible elongated and curved structure. The special features of the vessel structure lead, naturally, to consider the use of flexible computer vision models (snakes). Snakes [7] are of great interest since they are non rigid and have a physical explanation, where the energy principles are used to deform a curve under external forces coming from the image features. The weak point is precisely those external forces, usually computed by an edge or ridge detector and in a posterior step translated to a distance map simulating potential energy for curve deformation. Conventional image feature detectors, [1,2,3] are too general for the purpose of vessel detection in angiography bringing too many false responses that makes difficult the image interpretation. Even more, specific detectors are not good enough to discriminate

the vessel appearance [4,5,6]. Level set based ridge/valley detectors [3] offer a very good response but they could be strongly affected by the cleaning steps because in noisy images it is not guaranteed the continuity of the detected ridge/valley, i.e. the detected feature can suffer discontinuities along its path. When many holes are present in the path and each consecutive segment length is shorter than the proposed threshold, one can lose a very long part of the desired feature. The immediate consequence of large gaps in image features of interest is the distraction of the snake usually to near, false segments coming from image noise. Figures 1(a) and (b) illustrate the problem (original image is given in figure 4 (a)). The method inherits the properties of the detector. To avoid the problems commented above a learning process allows obtaining an accurate statistical description of the object (vessel) to assist the detection process. Such description has to be flexible enough to cope with vessel variability. With the knowledge accumulated in the learning process the external forces for the snake deformation can be described through a probabilistic potential map. Another approach is to embed the knowledge of the vessel profiles into the energy minimizing process of the snakes.

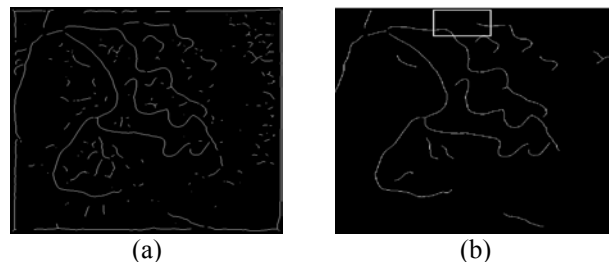


Figure 1. Crease detection (a) and post-processing of crease map (b).

2. A Probabilistic Framework for Structure Learning

The statistical approach is currently used in computer vision to add knowledge in different tasks from feature extraction to tracking [10, 11]. The first step is, usually, learning a feature of interest. For the vessel detection purpose, we propose two methods:

1. learning gray level profiles of the elongated structure;

- learning contrast coherence of the image feature and of a set of derivatives.

Learning grey level profiles

A descriptor representation by local grey-level image profiles perpendicular to the vessel elongation and longer than the maximal expected linear structure width is defined (fig.2).

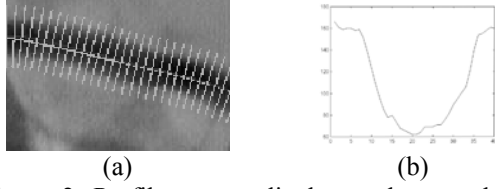


Figure 2. Profiles perpendicular to the vessel (a) and grey-level values of a profile (b).

To obtain the training samples, a "classic" snake [7] that deforms on a potential generated by a crease based distance map and corrected by the user (if necessary) is utilised. Each profile is defined by an image co-ordinate point (i, j) at the centre of the structure and a direction \mathbf{v} that indicates its orientation. The learning process is done by choosing the central points (i, j) and orientation of profiles \mathbf{v} from the snake position.

Let \mathbf{U}, \mathbf{V} be vectorial spaces referred to the image co-ordinates (i, j) and to the orientations \mathbf{v} respectively, where $(i, j) \in \mathbf{U}$ and $\mathbf{v} \in \mathbf{V}$. Then, we define a mapping:

$$T: \mathbf{U} \times \mathbf{V} \rightarrow \mathfrak{R}^d,$$

relating each extended co-ordinate pair and orientation $(i, j; \mathbf{v}) \in \mathbf{U} \times \mathbf{V}$, to a grey-level profile:

$$\tau_n \in \mathfrak{R}^d: \tau_n = T(i, j; \mathbf{v})$$

$$\tau_n = \{\tau_{n,k}\}_{n=1, \dots, N, k=1, \dots, d}$$

where n corresponds to the index of a pixel on the vessel centreline and k is a profile sample. By sampling the training set of images with a profile length d enough to cover the widest structure, we obtain a learning data set $D = \{\tau_1, \dots, \tau_N\}$. All profiles are aligned in order to obtain as far as possible axial symmetry with respect to the middle structure point. An interesting consequence of such an alignment is that the maximal probability shall be assigned to the real crease of the elongated object. Actually, vessel profiles are characterised by a high degree of statistic regularity due to their morphological consistency.

Learning contrast coherence

The intrinsic image structure in a coronary angiography leads us to consider the contrast coherence as a parameter to reinforce an accurate vessel description.

Direction of grey-level variance (Structure detection)

The structure tensor field, applied to an integration region ρ , of the regularized gradient image (∇I_σ) , under a suitable scale σ , measures the similarity between the regions and the searched structure [9].

Let K_ρ be a gaussian function as follows:

$$K_\rho = (1/2\pi\rho) \exp\{-(|x|^2 + |y|^2)/2\rho^2\} \quad (1)$$

and I an image under analysis. The so called structural tensor is defined as follows:

$$J_\rho = K_\rho * (\nabla I_\sigma \nabla I_\sigma^T) \quad (\rho \geq 0) \quad (2)$$

$$J_\rho = \begin{pmatrix} j_{11} & j_{12} \\ j_{21} & j_{22} \end{pmatrix} \quad (3)$$

where the $*$ in (2) means the convolution operator, ∇ the gradient operator and I_σ an image previously smoothed with a gaussian with standard deviation σ as follows:

$$I_\sigma(x, t) = (K_\rho * I(\cdot, t))(x) \quad (4)$$

The eigenvalues $\mu_{1,2}$ of the tensor J_ρ , ($\mu_1 \geq \mu_2$) describe the average contrast variation in the Eigenvectors $\mathbf{w}_{1,2}$ ($\mathbf{w}_1 \perp \mathbf{w}_2$). The following equations show the formulae to compute the eigenvalues and the eigenvectors:

$$\mu_{1,2} = \frac{1}{2}(\text{tr}(J_\rho) \pm \sqrt{\text{tr}^2(J_\rho) - 4\det(J_\rho)})$$

$$\text{tr}(J_\rho) = j_{11} + j_{22}$$

$$\det(J_\rho) = j_{11} * j_{22} - j_{12} * j_{21}$$

$$\mathbf{w}_1 = \{\cos \varphi, \sin \varphi\}$$

$$\tan 2\varphi = 2j_{12}/(j_{11} - j_{22})$$

The eigenvector \mathbf{w}_2 associated to the lower eigenvalue μ_2 , is the orientation of the lowest fluctuation, detecting the vessel flow (see fig. 3(a)). The first eigenvector describes the direction of maximal grey-level variance, e.g. the direction coincident with the one used to learn the profiles, fig. 3(b).

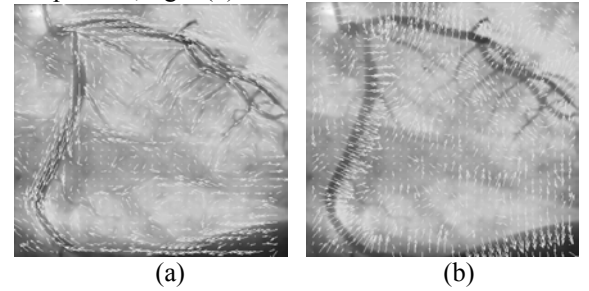


Figure 3. Eigenvectors associated with the lowest (a) and the largest (b) eigenvalue.

Not only the eigenvectors provide useful information. Areas with straight edges give $\mu_1 \gg \mu_2 \geq 0$, and corners give $\mu_1 \geq \mu_2 \gg 0$. A normalised coherence measure of local image structure is obtained as follows [9]:

$$\kappa = \frac{(\mu_1 - \mu_2)}{(\mu_1 + \mu_2)} = \frac{((j_{11} - j_{22})^2 + 4j_{12}^2)}{(j_{11} + j_{22})^2} \quad (5)$$

The potential discontinuity corresponding to flat image neighbours ($\mu_{12} \rightarrow 0$) is not a problem in our case

because the equality is true only in areas where the image is flat (constant). The possible limit case $\kappa \rightarrow 1$ because $\mu_2 = 0$ and $\mu_1 \rightarrow 0$ is eliminated by a next step through the likelihood.

The normalised coherence measure allows to focus on regions of interest with significant value of the coherence measure κ reducing, in this way, the computational cost of generation of a likelihood map for snake minimisation.

The coherence measure shall be used for:

1. The projection of the gaussian filters along the direction of contrast coherence and sampling the filter responses at the features of interest (vessels).
2. To constrain the degrees of freedom of orientation profile vectors \mathbf{v} , since they can be searched from the vector field \mathbf{w}_1 with the biggest structural tensor eigenvalue (fig. 1b).

Derivative Projections

A bank of Gaussian derivative filters $d^k K_\rho / d_x^{k_1} d_y^{k_2}$ at different scales ρ is used to obtain the statistic vessel description (K_ρ is defined in (1)). Note that different scales are necessary to cope with the vessel diameter variability while using different derivatives allows us to generalise edge, crest and valley detectors. Let us define a mapping of the image pixels to the space of filter responses:

$$I \rightarrow \mathcal{R}^n(x,y) \rightarrow \mathbf{F}(f_1, \dots, f_n) \quad (6)$$

Each sample f_i is a filter output $\mu_{k\rho}$ in a vessel pixel oriented by the eigenvector \mathbf{w}_1 :

$$\begin{aligned} \mu_{k\rho}(x,y) &= (d^k K_\rho / d_x^{k_1} d_y^{k_2}) * \mu(x,y) \quad k = k_1 + k_2 \quad (7) \\ f_i &= \mu_{k\rho}(x,y) \bullet \mathbf{w}_1 \quad i = 1, \dots, n \end{aligned}$$

A matrix $\mathbf{D}_{m \times n}$ is built where each row is a sample along the vessel. Given a set of training points (fig. 4(a)) we get their filter responses f_i , $i=1 \dots n$ and construct the training data matrix. In fig. 4(b) first derivative projection with $r = 9$ is shown. Fig. 4(c) depicts a training data matrix for the points in figure 4(a). The images were normalised to a gray level range $[0,1]$. The vertical axis in figure 4(c) corresponds to the filter outputs, axis x represents the learned points (rows of \mathbf{D}) and axis y represents the filters applied to each vessel point (columns of \mathbf{D}).

3. Vessel detection embedding a Mahalanobis distance into the minimising scheme: *eigensnakes*

We propose a new formulation of the energy-minimizing scheme called *eigensnakes* to allow statistically learning and detecting image features characterizing different appearances of non-rigid elongated objects. Incorporating the statistical framework, the approach can be extended to the labeling task and to obtain the whole coronary tree using a likelihood matching.

The eigensnakes comprises the learning, dimensional reduction and minimising scheme.

Dimensional reduction. Principal Component Analysis (PCA)

The use of PCA in this work is mainly for searching for a few optimal linear combinations of filters representing the dimensionality of the feature space. The optimisation in our case is in the sense of keeping the

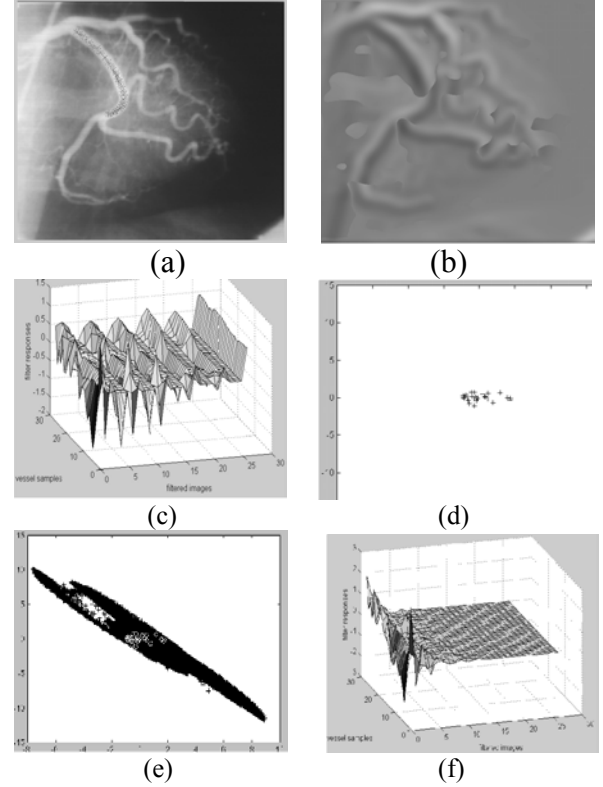


Figure 4. Training vessel samples (a). First Derivative directed by the first eigenvector of the image structure tensor (b). Learned data matrix (c). Learned cluster (d). Image projection (e). Representation of training image features in the feature space determined by principal axes (f).

set of variables explaining almost all the variance of the data and discarding the less important ones. Using PCA, a dimensional reduction is carried out as follows:

$$\Lambda: \mathcal{R}^n \rightarrow \mathcal{R}^l, l < n, \mathbf{f} \rightarrow \mathbf{y}$$

To obtain the principal components, the eigenvectors of the covariance matrix \mathbf{S} of $\mathbf{D}_{m \times n}$ are computed. The eigenvectors are sorted according to their associated eigenvalues (variances) and form the columns of a matrix \mathbf{W} . Such reduced space is used to measure the distance of an image feature to the learned ones. The measure can be regarded as a likelihood function giving the probability of each pixel belonging to a vessel category. Fig. 4(d) shows the training data projected onto the first two eigenvectors. Fig. 4(e) shows all image features projected onto the first two eigenvectors, the center of the cluster contains the learned data of fig 4(d). Fig. 4(f) shows the learned data projected onto the principal component co-ordinate system after dimensional reduction.

A probabilistic energy-minimising scheme

The aim is to make the snake to be attracted by image features corresponding to the statistical description of the object. To this purpose, the external energy of the snake is defined as a function of the Mahalanobis distance of the projected image features \mathbf{x} to the centre $\boldsymbol{\mu}$ of the learned cluster. The Mahalanobis distance [12] is computed in the reduced feature space, defined as follows:

$$E_{\text{ext}}(\mathbf{v}) = D_1^2(\mathbf{v}, \boldsymbol{\mu}) = (\mathbf{WFI}(\mathbf{v}) - \boldsymbol{\mu})^T \Lambda^{-1} (\mathbf{WFI}(\mathbf{v}) - \boldsymbol{\mu}) \quad (8)$$

where Λ is a diagonal matrix containing the eigenvalues of the training covariance matrix and $\mathbf{I}(\mathbf{v})$ is a vector representation of the image neighbourhood around the snake pixels.

Given that the internal energy associated to a snake implemented with a b-spline [18] is:

$$E_{\text{int}}(\mathbf{Q}(u)) = K_1 \alpha(u) |d\mathbf{Q}(u)/du|^2 + K_2 \beta(u) |d^2\mathbf{Q}(u)/du^2|^2$$

where $\mathbf{Q}(u)$ is a b-spline curve with parameter u , K_1, K_2 are constants and $\alpha(u), \beta(u)$ are functions representing the elasticity of the curve. Using the gradient of the probabilistic external energy in (8), we get a new energy minimising scheme for the snake:

$$-d/ds (\alpha v_s) + d^2/ds^2 (\beta v_{ss}) + (\cos \varphi, \sin \varphi) dD/de_1 = 0 \quad (9)$$

where $dD/de_1 = (\mathbf{WFI}(\mathbf{v}) - \boldsymbol{\mu})^T \Lambda^{-1} (\mathbf{W} d\mathbf{F}/de_1 \mathbf{I}(\mathbf{v}))$ and $\mathbf{e}_1 = (\cos \varphi, \sin \varphi)$ is the first eigenvector.

4. Vessel detection using feature profiles and Probabilistic Principal Component Analysis (PPCA)

In the PPCA framework [13, 14] a small number of causes are considered, that acting in combination generate the complexity of the observed data set. This leads to define a joint distribution $p(\mathbf{t}, \mathbf{x})$ over visible \mathbf{t} and distribution $p(\mathbf{x}, \mathbf{f})$ over visible $\{\mathbf{x}\}$ and hidden variables $\{\mathbf{f}\}$ the corresponding distribution $p(\mathbf{x})$ for the observed data is obtained by marginalization:

$$p(\mathbf{x}) = \int p(\mathbf{x} | \mathbf{f}) p(\mathbf{f}) d\mathbf{f}$$

The main goal is to find the parameters that maximise the joint observed data distribution i.e. the best description under a specific generative model.

One of the basic tools is the standard factor analysis [15], which seeks to relate d -dimensional observed data vectors $\{\mathbf{x}_n\}$ corresponding to a set of q -dimensional latent variables $\{\mathbf{f}_n\}$ by a linear mapping ($\mathbf{x} = \Gamma \mathbf{f} + \mathbf{n} + \boldsymbol{\mu}$) where latent variables are distributed into an isotropic Gaussian distribution, $\sim \mathcal{N}(0, \mathbf{I})$. The noise model \mathbf{n} , or error, is considered also Gaussian such that $\mathbf{n} \sim \mathcal{N}(\mathbf{0}, \Psi)$. The $(d \times q)$ parameter matrix Λ contains the factors loading, and $\boldsymbol{\mu}$ is a constant which, maximised the likelihood, corresponds to the mean $\boldsymbol{\mu}$ of the data. Given this formulation, the model for \mathbf{x} is also normal $\sim \mathcal{N}(\boldsymbol{\mu}, \Sigma)$, with mean $\boldsymbol{\mu}$ and covariance matrix $\Sigma = \Lambda \Lambda^T +$

Ψ . The corresponding probability density function is as follows:

$$p(\mathbf{x} | \boldsymbol{\mu}, \Sigma) = (1/(2\pi)^{d/2} \sqrt{\det \Sigma}) \exp(-1/2(\mathbf{x} - \boldsymbol{\mu})^T \Sigma^{-1} (\mathbf{x} - \boldsymbol{\mu})) \quad (10)$$

Assuming uniformly distributed noise over the whole image and linearity assumption in ($\mathbf{x} = \Gamma \mathbf{f} + \mathbf{n} + \boldsymbol{\mu}$) lead to the developing of a PPCA [13]. In this case Ψ endows with equal variance the principal axes (i.e. $\Psi = \sigma^2 \mathbf{I}$). Hence, PPCA is a permissible technique when illuminant variations problem is not analysed from variance structure. Considering this key assumption leads to consider the *conditional independence* of observed data. The underlying idea is that the dependencies between data variables \mathbf{x} are explained by a small number of latent variables \mathbf{f} , while \mathbf{n} represents the unique variance of each observation variable. Instead, conventional PCA treats both variance and covariance identically. The corresponding distribution of observed data ($D = \{\mathbf{x}_1, \dots, \mathbf{x}_N\} / \mathbf{x}_n \in \mathfrak{R}^d$) defines a normalised measure of distance, in a natural way, in terms of log-likelihood:

$$L(\boldsymbol{\mu}, \Sigma) = -\log p(D | \boldsymbol{\mu}, \Sigma) \quad (11)$$

This measure called *normalised Mahalanobis distance* reduces the penalty on pattern differences along cluster major directions of data distribution, instead of the Euclidean distance [16]. At this point, the problem is centred on parameter estimation, which, in practice, will be given by data observations. This leads to consider the problem of *incomplete data*. For this purpose, Dempster et al. in [17] use the EM algorithm, where each observation \mathbf{x}_n is associated to a unobserved state \mathbf{f}_n , and the main goal is to determine which component generates the observation. In this sense, the unobserved states can be seen as *missing data* and therefore the union of observations \mathbf{x}_n and \mathbf{f}_n is said to be complete data, $\mathbf{y}_n = (\mathbf{x}_n, \mathbf{f}_n)$. In this way the likelihood measure to be maximised is the *Complete-log-Likelihood*,

$$L = \sum_{n=1}^N \log p(\mathbf{x}_n, \mathbf{f}_n).$$

Maximum-likelihood formulation for PPCA also allows a closed solution for the mapping matrix Γ and the noise variance σ [13]:

$$\Gamma = U_q \sqrt{(\Delta_q - \sigma^2 \mathbf{I})} \mathbf{R}; \quad \sigma^2 = (1/d - q) \sum_{j=q+1}^d \delta_j \quad (12)$$

where U_q are the first q eigenvectors of the data set covariance matrix, Δ_q is a diagonal matrix with the corresponding first q eigenvalues ($\delta_i, \forall i, 1 \leq i \leq N$) and \mathbf{R} is an arbitrary rotation matrix.

Ought to the high number of pixels (samples) in any image, a dimensional space reduction by means of PPCA is used to statistically describe the feature.

Each sample is a grey-level profile and the covariance matrix S of the observed data is constructed from the learning data set:

$$S = (1/N) \sum_{n=1}^N (\mathbf{t}_n - \boldsymbol{\mu})(\mathbf{t}_n - \boldsymbol{\mu})^T,$$

where N corresponds to the profile population, $\boldsymbol{\mu}$ is the sample mean profile and \mathbf{t}_n is the n -th grey-level profile.

The diagonalization of the covariance matrix S allows to reach the closed solution for the maximum likelihood estimation in (12). Hence, it provides the transformation between latent variables and observed data as a linear mapping $\mathfrak{R}^q \rightarrow \mathfrak{R}^d$, being q the latent space dimension and d the profile length, defined by the projection matrix Γ and the sample mean $\boldsymbol{\mu}$.

Feature detection

At this stage, the main goal is to build a local likelihood map for the snake given the image neighbourhoods projected onto the optimised space \mathfrak{R}^d . The mapping is a probability measure of belonging to the learned structure category $\Omega = (\Sigma, \boldsymbol{\mu})$ for each co-ordinate pixel (i,j) and any direction \mathbf{v} . Since the learned model is done through the grey-level profiles, the following functional composition to build the likelihood map $P(T(i,j;\mathbf{v}) | \Omega)$ is defined:

$$U \times V \rightarrow \mathfrak{R}^d \rightarrow \mathfrak{R} \\ (i,j;\mathbf{v}) \rightarrow \mathbf{t} \rightarrow P(T(i,j;\mathbf{v}) | \Omega)$$

Computing this probability requires a factorisation of the model covariance matrix: $\Sigma^{-1} = (WW^T + \sigma^2 I)^{-1}$. This can be done with low computational cost (i.e. $O(q^3)$ instead of $O(d^3)$) using the Woodbury's identity:

$$(WW^T + \sigma^2 I)^{-1} = \{ I - W(W^T W + \sigma^2 I)^{-1} W^T \} / \sigma^2$$

In order to detect the learned feature, the image under analysis ought to be scanned searching profiles like the learned ones. Hence, the main problem arises when it comes to assign for each pixel (i,j) the profile orientation \mathbf{v} . However, due to the elongated structure of the objects it is not necessary to learn any curve shape or to scan the image considering all directions. Instead, the profiles are oriented with the direction of maximal grey-level variance of image neighbourhood by a structure tensor [9]. Since profile orientation \mathbf{v} is fixed for each pixel (i,j) , the profile extraction is done through the mapping:

$$(i,j;\mathbf{v}) \rightarrow \mathbf{t} = T(i,j;\mathbf{v}).$$

Then the distance map from every profile to the learned model is obtained as a result of assigning its corresponding negative log-likelihood defined in (11) to each pixel. The minimal probability computed in the regions of interest is assigned to all areas discarded by the threshold on the coherence measure k (5).

Hybrid Snake Potential

The obtained likelihood map offers high responses (i.e. negative likelihood tends to -1 in image features of interest) at centrelines of elongated objects and nearby forms strong slope towards the centreline. As a result, good convergence behaviour is observed once the snake falls in a neighbourhood of the elongated structure. Another advantage of the refined map is the small amount of false responses (potential points with high probability to represent learned feature and at the same time not belonging to an elongated structure).

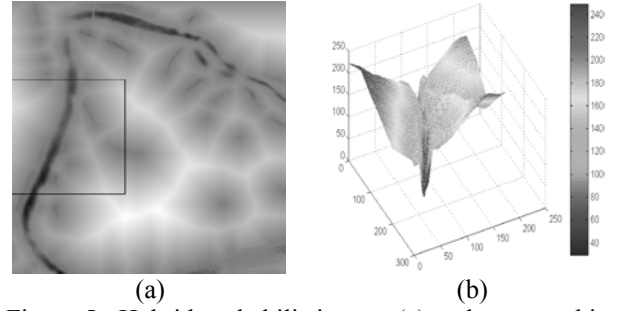


Figure 5. Hybrid probabilistic map (a) and topographic map (b) of a part of the hybrid potential shown by the black square in (a).

Therefore, far from the objects of interest the potential map consists of large flat areas with constant 0 likelihood. In these regions, a snake (initialised far from the objects of interest) does not suffer any external forces to deform it. It is more effective having a smooth slope towards the feature. To cope with these plain areas, the negative likelihood map is enhanced:

$\hat{p}(\mathbf{x} | \Omega) = -p(\mathbf{x} | \Omega)$ obtaining a hybrid potential field as follows:

$$P_{\text{hybrid}}(\mathbf{x} | \Omega) = \{ \hat{p}(\mathbf{x}), \hat{p}(\mathbf{x}) \in [-1, 0) \} \\ P_{\text{hybrid}}(\mathbf{x} | \Omega) = \{ d(\mathbf{x}), \text{ otherwise} \}.$$

where $d(\mathbf{x})$ is the distance to the closest potential point with non-zero probability. As a result, the snake moves with a constant small step towards the potential zones and converges only to the zones corresponding to learned image features. Fig. 5(a) illustrates the hybrid map and fig. 5(b) a topographic map corresponding to the black square in 5(a). As a result, the likelihood map is modified to avoid the uncertainty regions far from the detected feature using a distance function to the high likelihood regions.

5. Conclusion

The value of the statistic basis for linear structure detection has been established by demonstrating two methods:

1. The mechanism of PCA and Mahalanobis distances embedded into the minimisation scheme of the snakes.
2. The mechanism of the PPCA embedded into the snake framework.

Snake-based feature detection of image structures is based on the minimization of a functional energy term, which is usually created from the outcome of a standard feature detector. This fact constrains the applicability of the method and reduces the classes of image structures that can be analyzed. In order to manage complex objects and the variability of appearance of image structures, our techniques are supported by a learning approach to extract and detect only these "crease-like" features determined by the training set. Learned models are used in a probabilistic framework in order to build significant energy potential, resulting in less false responses of the image feature detector and more robust snake-based object segmentation.

A new approach to potential computation using a likelihood map is formulated and applied to the tracking of specific structure on angiographies: coronary vessels as a difficult example of automatic analysis. As a result, the snake is less dependent on its initialization and once placed on the hybrid potential map it converges to image features with high probability to represent learned object profiles. The obtained results and the self-training capability of the snake encourage utilizing it in different applications. Finally, the experiments carried out showed that there are no significant differences between the use of PCA or PPCA regarding the results (vessel detection). The PCA are faster to compute, meanwhile PPCA offers a probabilistic framework open to incorporate higher levels of reasoning.

6. Acknowledgments

This work was partially supported by "Ministerio de Ciencia y Tecnologia" grant TIC2000-1635-C04-04.

References

- [1] R. Poli, G. Coppini, M. Demi, and G. Valli. An artificial vision system for coronary angiography. *Proc. Computers in Cardiology*, 1991, 17-20.
- [2] X. Zhang, S. M. Collins, and M. Sonka. Tree pruning strategy in automated detection of coronary trees in cineangiograms. *Proceedings of International Conference on Image Processing ICIP'95 IEEE*, 1995, 17:656-659.
- [3] A. Lopez, R. Toledo, J. Serrat, and J. J. Villanueva. Extraction of vessel center-lines from 2d coronary angiographies. *Proc. of the 8th National Conference on Pattern Recognition and Image Analysis*. Bilbao, Spain, 1999, vol 1. no. 11:489-496.
- [4] Y. Sun. Automated identification of vessel contours in coronary arteriograms by an adaptive tracking algorithm. *IEEE Transactions on Medical Images*, 8:78-88, 1989.
- [5] A. C. M. Dumay. *Image Reconstruction from Biplane Angiographic Projections*. PhD thesis, Technische Universiteit Delft, Netherlands, 1992.
- [6] K. Barth, B. Eicker, and J. Seissl. Automated biplane vessel recognition in digital coronary angiograms. *Proceedings SPIE. Medical Imaging IV. Image Processing*, 1990, 1233:266-274.
- [7] M. Kass, A. Witkin, and D. Terzopolous. Snakes: Active contour models. *International Conference on Computer Vision*. London, 1987, 259-268.
- [8] P. Radeva, J. Serrat, and E. Marti. A snake for model-based segmentation. *International Conference on Computer Vision*. MIT. USA, 1995, 816-821.
- [9] J. Weickert. Coherence-enhancing diffusion of color images. *Image and Vision Computing*, 1999, 17:201-212.
- [10] G. J. Edwards, C. J. Taylor, and T. F. Cootes. Learning to identify and track faces in image sequences. *British Machine Vision Conference*, 1997, 8:130-139.
- [11] A. Blake and M. Isard, editors. *Active contours*. (Springer Verlag, 1998).
- [12] K. V. Mardia, J. T. Kent, and J. M. Bibby, editors. *Multivariate Analysis*. (Academic Press. Harcourt Brace & Company Publishers, 1995).
- [13] Christopher M. Bishop and Michael E. Tipping. *Probabilistic principal component analysis*. Tech. Report NCGR, 1997.
- [14] Christopher M. Bishop and Michael E. Tipping. *Mixtures of probabilistic principal component analysers*. Technical Report NCGR, 1998.
- [15] D.J. Bartholomew. *Latent Variable Models and Factor Analysis*. Charles Griffin and Co. Ltd., 1987.
- [16] K. Sung, Tomaso Poggio. *Example-based learning for view-based human face detection*. A.I. Memo 1521, C.B.C.L. , 1994, Paper 112.
- [17] A.P. Dempster, N.P. Lair, and D.B. Rubin. *Maximum likelihood from incomplete data via the EM algorithm*. 39 *Journal of the Royal Statistical Society Series B*, 1977, 1-38.
- [18] R. Toledo. Cardiac Workstation and Dynamic model to assist in Coronary Tree Analysis. PhD Thesis, Ediciones Gráficas Rey SL, 2001, 39-53.